

Article

Formation of Abnormal Gas-Geochemical Fields and Dissolved Gases Transport at the Shallow Northeastern Shelf of Sakhalin Island in Warm Season: Expedition Data and Remote Sensing

Nadezhda Syrbu ^{*}, Andrey Kholmogorov , Igor Stepochkin , Vyacheslav Lobanov  and Svetlana Shkorba

V.I. Il'ichev Pacific Oceanological Institute FEB RAS, 690041 Vladivostok, Russia;
kholmogorov.ao@poi.dvo.ru (A.K.); stepochkin.ie@poi.dvo.ru (I.S.); lobanov@poi.dvo.ru (V.L.);
sshkorba@yandex.ru (S.S.)

* Correspondence: syrbu@poi.dvo.ru

Abstract: Our paper deals with gas-geochemical measurements of CH₄ and CO₂, as well as the first measurements of dissolved H₂ and He in the waters of the eastern shelf of Sakhalin Island, obtained during cruise 68 on the R/V Akademik Oparin (OP68) on 12–18 August 2023. The shallow eastern shelf has high concentrations of dissolved methane and helium in the water. The combined anomalies of methane and helium indicate the presence of an ascending deep fluid. The sources of methane in the studied area are the underlying oil- and gas-bearing rocks extending to the coast of the island. The deep faults of the region and the minor discontinuities that accompany them along the eastern coast of Sakhalin Island create a fluid-permeable geological environment both on the shallow shelf and on the coastal part of the island. East Sakhalin current and counter-current influence gases that migrate from lithospheric sources; these currents form a special hydrological regime that ensures high solubility of the gases released and their transfer under the lower boundary of the seasonal pycnocline to the east, where they are involved in the general circulation of the Sea of Okhotsk.

Keywords: methane; helium; hydrogen; sea currents; transport; oil and gas content; gas geochemistry; northeast shelf of the Sakhalin Island



Citation: Syrbu, N.; Kholmogorov, A.; Stepochkin, I.; Lobanov, V.; Shkorba, S. Formation of Abnormal Gas-Geochemical Fields and Dissolved Gases Transport at the Shallow Northeastern Shelf of Sakhalin Island in Warm Season: Expedition Data and Remote Sensing. *Water* **2024**, *16*, 1434. <https://doi.org/10.3390/w16101434>

Academic Editor: Cesar Andrade

Received: 5 April 2024

Revised: 9 May 2024

Accepted: 12 May 2024

Published: 17 May 2024



Copyright: © 2024 by the authors. Licensee MDPI, Basel, Switzerland. This article is an open access article distributed under the terms and conditions of the Creative Commons Attribution (CC BY) license (<https://creativecommons.org/licenses/by/4.0/>).

1. Introduction

Continental margins constantly attract the attention of researchers. Their study is not only relevant from the perspective of studying modern active geological processes and oil and gas potential but also related to the problem of studying gas-geochemical parameters in the seas and land-shelf transit zones.

The most active lithosphere degassing occurs within the Hokkaido–Sakhalin folded system in the Okhotsk Sea region. The Sakhalin region encounters great interest from the standpoint of the genesis and ecological significance of natural gases contained in sedimentary basins, accumulations of underwater gas hydrates, geothermal and mud volcanic systems, gas-saturated groundwater, and marine sediments [1].

The shelf of the Hokkaido–Sakhalin folded region is a direct extension of the land according to its genesis [2,3]. Almost all ridge–mountain land relief elements having distinct morphological extensions in the form of underwater uplifts within the shelf evidence this. The main deep faults of the shelf zone are extensions of tectonic disturbance zones of the land area. This is especially evident in the area of the border between the Amur and Eurasian lithospheric plates in the Sakhalin Island area (Figure 1).

Modern tectonic studies consider the structure of the East Asian continental margin as being such that it is formed by a complex combination of accretion and collision processes in space and time, as well as transformative movements of both individual terranes and their ensembles [4–8]. Currently, the relationship between the formation of the geological structure of Sakhalin Island and adjacent waters with the development of Phanerozoic

active Pacific margins is considered proven [2–5,9]. The transverse tectonic zonality of the folded system is well expressed. It runs from the southern parts of Hokkaido Island to the Schmidt Peninsula in the north of Sakhalin Island.

In this regard, underestimation of the continental and coastal shelf parts of the marginal seas leads to an incomplete understanding of the distribution processes of gas-geochemical fields directly related to the main geological structures, tectonics, and hydrocarbon potential of the territory.

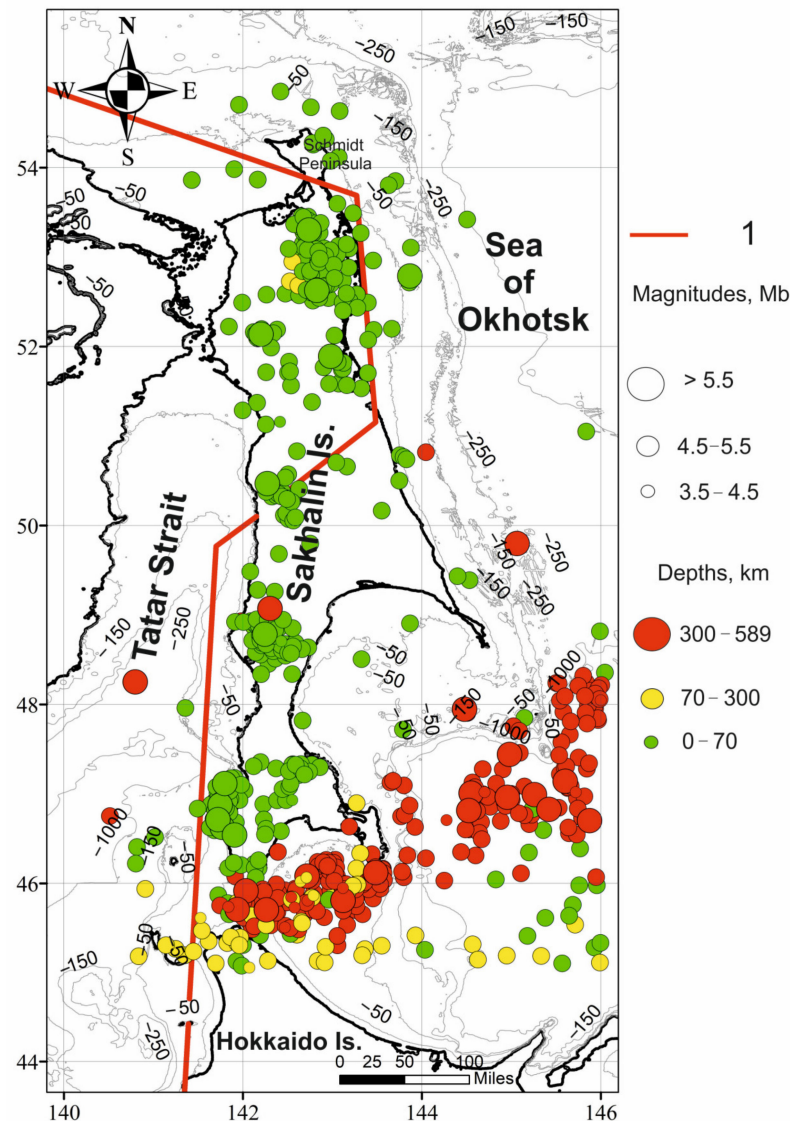


Figure 1. A scheme of the lithospheric plates in the Sakhalin region (according to [10]) and the distribution of seismicity for 1992–2023 [11]. 1—Boundary of lithospheric plates (deep shift).

The Sea of Okhotsk is one of the most active areas of underwater methane discharge in northern latitudes [1,12–14]. The elevated concentrations of methane in the water column of the marginal seas are usually possible due to active underwater gas emission [15–19]. Many studies [20–23] have established the genetic relationship of underwater methane emission with oil and gas deposits, gas hydrate accumulations, deep faults, surface ruptures, and folds for the marginal seas of the northwestern Pacific Ocean.

However, the issues of studying the complex geological and structural conditions of the underwater methane emission formation in the Sea of Okhotsk remain controversial and need additional research.

Gas emissions are usually associated with large and small movements of the Earth's crust, anticline uplifts, and mud volcanoes. Numerous gas seeps are associated with tectonic linear cracks, which manifest themselves in bottom sediments in the form of elongated linear anomalous zones for methane, its homologs, helium, hydrogen, and sometimes CO₂ [24,25]. Such anomalous zones have been found in many marine basins: for example, in a linear fault extending along the center of the Tatar Strait in the Japan Sea [26–29]. In our study, the concept of a gas anomaly is considered to be a concentration exceeding the background values by more than two times [1]. Methane emission on Sakhalin Island and the adjacent waters of the northeastern shelf of the Sea of Okhotsk can be conditionally divided into three types: (1) local methane emission (mud volcanoes, gas vents, gas hydrothermal vents, etc.); (2) areal methane emission over oil- and gas-bearing structures through a network of faults; and (3) areal methane emission in the erosion zone of folded structures.

Microbes oxidize approximately an equal amount of methane in the case of shallow shelf methane seeps (up to 100 m), and the other half is transferred to the atmosphere. At the same time, microbes at deep-sea local gas outlets oxidize most of the methane; vertical diffusion facilitates it and limits methane exchange in the mixed water layer and, consequently, the release into the atmosphere. As shown in [30], only one-quarter of the CH₄ released from the Coal Oil Point seep field undergoes microbiological oxidation, while the rest is transferred to the atmosphere through bubbles (one-half) and through gas exchange of marine air in an upper mixed water layer.

The study of the shallow oil- and gas-bearing northeastern shelf of Sakhalin Island allows us to increase the understanding of the processes of methane emissions in the Far Eastern marginal seas caused by geological sources. Methane emissions studies need a complex approach by integrating several disciplines—geology, oceanology, and geochemistry.

Several studies confirm that water circulation influences methane distribution. For example, methane carried into the waters of the North Sea by rivers is transported further by currents [31]. Studies in the Eastern Pacific Ocean conducted by F.J. Conner and A.A. Yayanos [32] also revealed that the increased CH₄ content in areas remote from the coast of California is due to the influence of the California Current.

The purpose of this paper is to discuss the relationship between the impact of the major geological and hydrometeorological factors on methane concentration and variability in the water column in the shallow oil- and gas-bearing northeastern shelf of Sakhalin Island.

Observations of seasonal changes in methane concentrations in the water columns will increase the reliability of calculating the contribution of methane coming from the water surface on the eastern shelf of Sakhalin Island to the atmosphere.

2. Materials and Methods

Gas-geochemical research aims to assess the variability of the methane content in seawater levels to identify the sources of gas emission as well as to obtain information for further assessment of the relationship of background and anomalous gas-geochemical fields with morphostructural and tectonic elements of the geological structure. Methane, carbon dioxide, hydrogen, and helium dissolved in water are indicators of fault zones and allow us to predict seismic activity, assess the state of the environment, and search for hydrocarbon deposits.

We use the results of research works conducted on the northeastern shelf of Sakhalin Island within cruise 68 on the R/V Akademik Oparin (OP68) during 12–18 August 2023. The main hydrocarbon accumulations of the region are located in the area of the northern fault of the Hokkaido–Sakhalin deep shift (Figure 1). We performed three oceanographic sections across the shift fault during the cruise.

Seawater was sampled by an SBE ECO-55 carousel with 4 L Niskin bottles during profiling of the SBE19 CTD in the depth range from the surface to the bottom, as well as from a flow water intake system at a level of 5 m (Table 1).

Table 1. Depth of water sampling (cruise 68 of R/V Akademik Oparin).

	Station				Depth			
Section 1 (northern)	17	303	281	238	202	72	26	4
	18	225	201	149	79	54	28	4
	19	161	134	85	85	62	34	4
	20	127	108	75	76	51	30	4
	21	67	58	46	45	26	15	4
Section 2 (central)	22	30	15	10	4			
	23	84	66	40	24	15	4	
	24	110	80	63	41	20	4	
	25	151	129	100	73	39	20	4
	26	182	164	140	99	60	18	4
	27	284	265	181	131	74	25	4
Section 3 (southern)	29	281	260	200	132	61	30	4
	30	140	121	91	61	30	16	4
	31	96	80	61	35	21	11	
	32	76	61	40	29	17	11	
	33	45	39	31	20	10	4	

The Headspace equilibrium concentration method [33] was used to analyze the content of methane, carbon dioxide, helium, and hydrogen in all samples. The water from the bottles was sampled into pre-sterilized medical glass bottles with a volume of 60 and 100 mL by the “triple overflow” method. Then, the bottles were hermetically sealed with sterile rubber stoppers without access to atmospheric air into the bottles. Needles from a medical syringe were used to remove excess water.

Helium (10 mL) grade 6.0 was equilibrium injected into the bottles to analyze carbon dioxide and methane content during the creation of the gas phase. Atmospheric air (10 mL) was equilibrium-injected into the bottles to analyze the content of helium and hydrogen. Further, the samples were intensively mixed. Before the analysis, the gas phase was equilibrium-extracted with a syringe to insert the sample into the gas chromatograph. The analysis of hydrocarbon gases, along with nitrogen, oxygen, and carbon dioxide, was carried out using a CristalLux 4000 M two-channel gas chromatograph equipped with particle flux and thermal conductivity sensors (sensitivity of $10^{-5}\%$). For helium and hydrogen analysis, a “Chromatec-Gazochrom 2000” (JSC “Chromatec”, Yoshkar-Ola) gas chromatograph with high-sensitivity thermal conductivity sensors (1–2 ppm for helium and hydrogen) was used. Components of the separable mixture were placed into a chromatographic column with a gas carrier (in our case, argon). The duration of each analysis lasted 5 min. When equilibrium between the liquid and gas phases was reached, the gas sample (5 mL) was taken by syringe for the chromatographic analysis. Errors in the helium and hydrogen determination were 0.03 and 0.02 ppm, respectively. Because the considered gases are readily volatile, samples were analyzed for 1 h after sampling, while samples prepared for analysis in stationary laboratories were conserved with chlorhexidine and preserved at +4 °C in darkness using a portable refrigerator.

The dissolved seawater methane, helium, and hydrogen concentrations were calculated according to the method described in [34], including a modification described in [35], using the calculated solubility constants of methane.

The work is based on research data obtained during expeditions to Sakhalin Island, as well as in the Sea of Okhotsk. The validation of the results is confirmed by a significant amount of research and the data convergence for gas concentrations and isotopic composition in different regions and by the data of predecessors.

The validation of gas analytical work is determined by the modern level of chromatographic equipment used, sampling methods and sample preparation, processing techniques, the research results and standards used, constants, and calculation algorithms.

The preparation of the samples and analytical studies were carried out according to the certified method adopted in the Gas Geochemistry Laboratory of the V.I.Ilichev Pacific Oceanological Institute, approved by the Federal Agency on Technical Regulating and Metrology (Certificate No. 58, Technical Data Sheet PS 1.051-21).

We analyzed the satellite monitoring data of the methane concentration in the air over the water surface on the Sakhalin northeastern shelf in the period of 15–16 August 2024 using data obtained by AIRS [36,37], which operates on the AQUA satellite (NASA, USA), conducting global sensing of the Earth's atmosphere. The scanner provides temperature, water vapor, and atmospheric methane profiles, as well as data on aerosol fractions in the form of images of the Earth's surface with a spatial resolution of 30 km.

3. Oceanographic Features of the Research Area

The East Sakhalin current (ESC) is a western section of the basin-scale cyclonic circulation gyre of the Sea of Okhotsk (Figure 2) [38,39]. In general, it carries water along the eastern shelf and the slope of Sakhalin Island in a southern direction [38–42]. The ESC transports cold and low-salinity water from the northwestern part of the Sea of Okhotsk, the most isolated area, where slowly melting floating ice stagnates until early summer. In summer, the ESC transports low-salinity water influenced by the Amur River discharge. The hydrological regime in this area is greatly influenced by the flow of the Amur River, the largest river in the Far East (annual volume is about 400 km³). The cold and heavy water of the ESC forms a dichothermal subsurface layer in the Sea of Okhotsk and propagates south to the Kuril Straits, where it contributes to ventilation of the North Pacific intermediate layer [43].

The average velocity of the ESC is 10–12 cm/s, and it may increase up to 20–40 cm/s in a high-tide phase [41]. The current has strong seasonal variability of its structure. Diagnostic quasi-geostrophic models [44,45] show a strong seasonal variability in the current and increase in the flow velocity to 40 cm/s in autumn and a weakening in summer.

Observational data, however, demonstrate quite a complex structure and variability in the ESC. Drifters and instrumental measurements of the currents carried out in 1998–2001 [46] show that ESC consists of two branches. One branch proceeds near the shore, over depths of 50–150 m and with velocity of 30–40 cm/s. The second is above the continental slope, with depths of 300–900 m and a velocity of 20–30 cm/s. Numerical modeling presented in [46–49] confirms this structure of the ESC in detail as well as satellite altimetry data [50], which also show seasonal and inter-annual fluctuations in the current.

The papers of [51,52] give the modeling results of the Sea of Okhotsk circulation for each month and various levels from the surface down to 500 m, demonstrating seasonal changes in the ESC velocity and direction, and the possibility of reverse flow, but its general mean direction from north to south is commonly recognized.

Mooring observations [53] and satellite data analysis [40] show that southern winds dominating in summer create a seasonal upwelling area along the Sakhalin coast with colder water coming up to the surface. The water temperature of the surface layer increases with distance from the coast, which usually leads to the formation of a counter-current outside the Sakhalin shelf, oriented to the north. ESC weakens in the coastal zone, and a flow of low-salinity water originating from the Amur River is blocked by the East Sakhalin counter-current (ESCC) and is hardly observed south of 52 °N.

An analysis of multi-year CTD observations (around 40 years) along hydrographic sections [54] shows that ESC and ESCC are the main and persistent elements of the water circulation on the northeastern shelf of Sakhalin Island. They are permanently present in every season, but their intensity varies significantly both in time and space [51,52,55]. During the October–May period, the ESC has its maximum velocities (up to 20 cm/s) and occupies the coastal part of the shelf 50–100 km off of the shoreline. Meanwhile, the ESCC is directed northward and located over the Sakhalin slope (deeper than 200 m) to the

east of the coastal branch of the ESC. Even in winter, both flows have velocities of up to 4–5 cm/s under the ice. During the summer season (July–August), the northern flow of ESCC occupies the whole shelf area up to 180 km off the shoreline with velocities of 15–17 cm/s and is observed down to a 200–250 m depth.

Strong tidal motion is an important component of water dynamics over the eastern shelf of Sakhalin Island [38–41]. Diurnal tides form shelf waves trapped at the northwestern shelf area [40]. This leads to mesoscale variations in the flows. The work [56] also shows the presence of mesoscale circulations features in ESC. The authors associate the formation of mesoscale eddies with coastal upwelling caused by northerly winds and positive wind stress along the Sakhalin coast. Such mesoscale cyclones and anticyclones provide water exchange between the shelf and the deep-water basin of the Sea of Okhotsk.

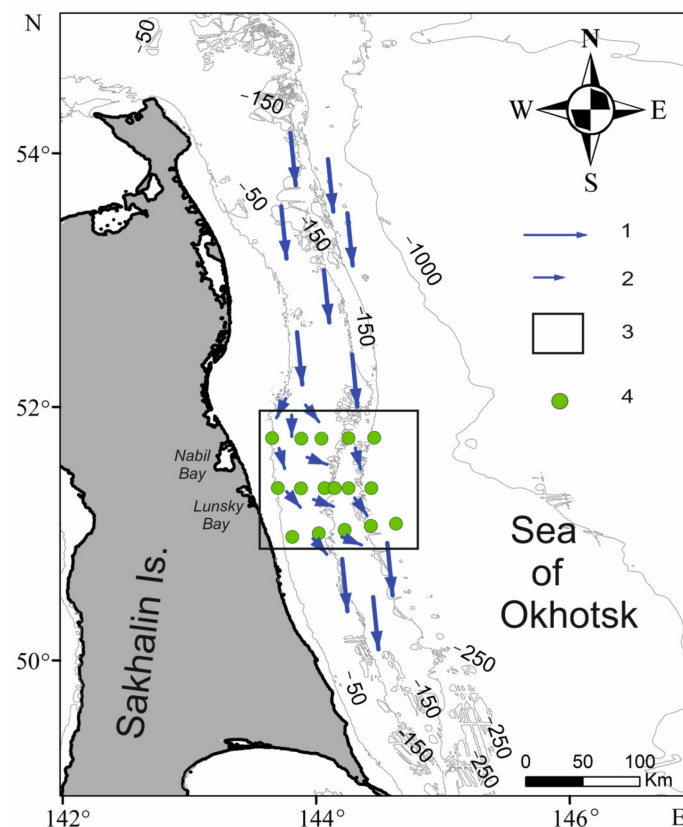


Figure 2. Scheme of the East Sakhalin current on the northeastern shelf of Sakhalin Island. 1—The main flow of the East Sakhalin current; 2—mesoscale fluctuations [56]; 3—the research area; 4—water sampling stations on cruise OP68, August 2023.

4. Geological Features of the Research Area

Sakhalin Island and its shelf are part of the Okhotsk Sea region, which in turn is part of the Asia-Pacific transition zone from the continent to the ocean. Geologically, the region is a giant interblock structure at the global level and an area of intense discharge of deep energy with active Late Mesozoic–Cenozoic and modern geodynamics [57].

The Hokkaido–Sakhalin fold system of the Late Mesozoic–Cenozoic is represented by the structural features of the islands of Sakhalin and Hokkaido, the connection between them being southern Sakhalin. Over the entire length of this fold system, its eastern segments, which represent a complex region connecting oceanic structural features and continental margin ones, provide good objects for reconstructing the evolution of the transition zone [9].

The western boundary of the Okhotsk lithospheric plate (see Figure 1) has been defined ambiguously, and its boundary is treated in different ways. Russian geophysicists [58,59]

pinpointed its location on Sakhalin Island, extending northwards through the Sea of Okhotsk. These concepts completely ignore the absence of earthquake foci, as well as regional and deep patterns of geological structures (for example, the arcuate shape of the Okhotsk–Chukchi volcanic–plutonic belt). The scheme adopted in our research (see Figure 1) is based on the fact that the western boundary of the plate runs almost north of Sakhalin Island along unambiguously fixed epicenters of earthquakes that turn west here. From the south of Sakhalin Island, the western border of the plate runs along the Tatar Strait to the west of the island. It crosses Sakhalin Island further in the middle part, where the structures of the Cretaceous pre-arc deflection are displaced along the Mesozoic transform fault [4,60]. Previously conducted gas-geochemical studies on Sakhalin Island confirm this position of the boundary of lithospheric plates. A boundary of lithospheric plates (deep shift) divided Sakhalin Island into two gas-geochemical provinces [61,62] (Figure 3).

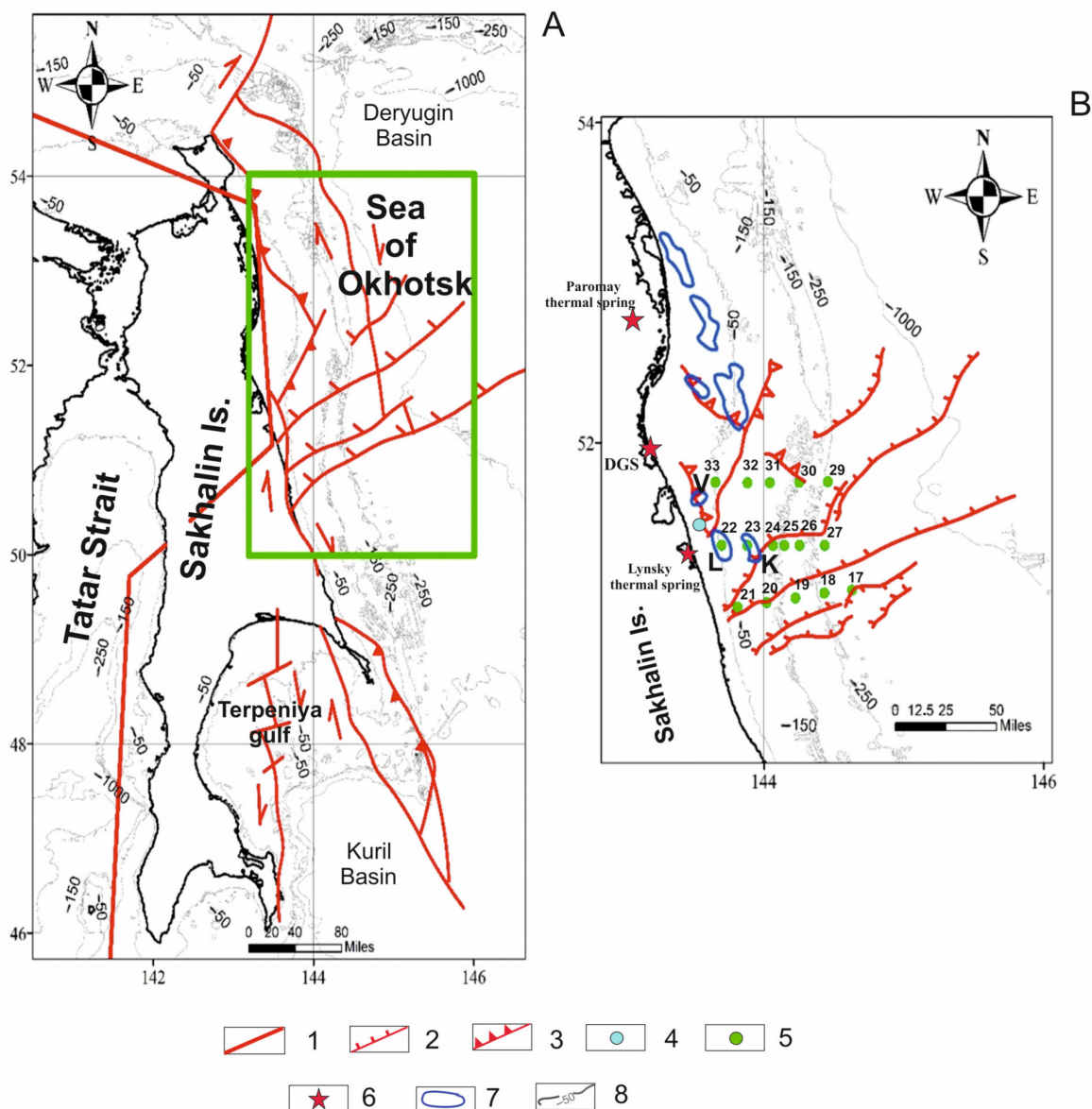


Figure 3. Scheme of the main faults of the eastern shelf of the Sakhalin Island slope (A) and a tectonic diagram of the central part of the eastern shelf research area (B) (according to [57,63,64]). 1—Boundary of lithospheric plates (deep shift); 2—reverse faults; 3—thrust faults; 4—Nicole “gas flare”; 5—water sampling stations (OP68); 6—thermal springs (DGS—Daginsky gas-geothermal system, Lunskey thermal spring, Paromay thermal spring); 7—gas condensate fields (L—Lunskey, K—Kirinsky, V—Veninskoe); 8— isobates.

According to a number of recent studies [65,66], the Okhotsk Plate, squeezed by the Eurasian, Amur, North American, and Pacific plates, rotates counterclockwise. This is also indirectly evidenced by right-sided tectogenesis in the zones of sublatitudinal lithospheric faults of the Okhotsk Sea Plate [57]. An analysis of the structural features of the sedimentary basins of the Okhotsk Sea region shows that the vast majority of them are controlled by tectonic deflections that developed under conditions of destructive tectogenesis. Destructive rifting processes ensured not only the formation of large sedimentary basins but also the creation of favorable conditions for the intensive formation, accumulation, and destruction of hydrocarbon accumulations. At the same time, rifts, being the most effective conductors of the Earth's deep heat, have formed not only a thermodynamic environment here optimal for the processes of oil and gas formation but, being the largest permeable structures of the lithosphere, serve as conductors of ascending fluid flows [57].

The deep structure of the Sakhalin region was formed by active geodynamic processes of the Late Mesozoic–Cenozoic and is characterized by dynamic fluid stratification of the lithosphere. Modern and active vertical fluid flow in the region is manifested in hydrocarbon accumulations, mud volcanoes, and thermal springs. The result of this process is also reverse folding. An indirect sign of vertical fluid migration is the multiplasticity of the Sakhalin hydrocarbon deposits. The main vertical migration routes are the weakest and most permeable thrust fault zones and the intersection with different orientations [57].

The entire Sakhalin region is located in a seismically active region and belongs to the Pacific Mobile Belt. Seismic activity is an indicator of the stress–strain state of the Earth's crust, which affects the processes of oil and gas accumulation. The epicenters of all earthquakes are associated with deep shifts [67]. Seismicity data indicate the important role of deep shifts in the formation of the geological structure of the island. The sphere of influence of deep faults at the time of tectonic movements extends over 60 km and is characterized by the greatest stresses in the fault zone of 3–4 km.

Vertical displacement amplitude along Hokkaido–Sakhalin and Central Sakhalin faults is 400–600 m. Earthquakes can initiate the mixing of deep fluids and their vertical migration through permeable zones in the area of deep tectonic deflections [68].

Fluids fill the cracks and can be squeezed up the fault. If a sedimentary cover (the northeastern part of the Sakhalin Island) blocks the fault, then fluids accumulate in layers of porous and fractured rocks. However, if the fault communicates with the earth's surface (the southern and southwestern parts of Sakhalin), then fluids come to the surface [62].

The research area is located in the central part of the eastern water area of Sakhalin Island within the North Sakhalin sedimentary basin, the length of which in the northwesterly direction is 900 km with a width of 80–120 km. This area corresponds to the North Sakhalin oil and gas region, which unites the promising basins of Northern Sakhalin, the adjacent waters of the Sakhalin Bay, and the northeastern shelf of Sakhalin Island.

Paleogene–Early Miocene riftogenic destruction formed the structure of the sedimentary strata of the North Sakhalin trough. The activation of tectonic movements in megadrive zones formed this sedimentary basin as a folded region (the northern link of the Hokkaido–Sakhalin folded system) at the end of the Neogene period. The structure of the trough is complicated by predominantly meridional and latitudinal tectonic disturbances and large gently dipping folds of the north-northwest and submeridional orientations [57].

The following types of methane or methane-containing fluids are currently known in the North Sakhalin trough: shallow-water single seeps, mud volcanoes, methane seepage through fault zones above oil and gas-bearing structures, surface oil, and gas occurrences on Sakhalin Island.

Four seeps were found within the North Sakhalin sedimentary basin, located in a submeridional direction at a great distance from each other at depths up to 100 m and confined to the Northeastern Sakhalin Trough [69–71].

The Nicole “gas flare” (depth 40 m) is mapped within the Lunsky gas condensate field, which is an anticline fold broken into blocks by faults, which creates favorable conditions for gas emission. Here, during the monitoring, a stable methane anomaly with a concentration

of about 500–3000 nL/L was fixed (22.3–134 nM/L). Other seeps were also recorded within the East Sakhalin fault zone directly above the oil- and gas-bearing structure. In the area of seeps, methane anomalies have been found from about 1000 nL/L on the surface (44.6 nM/L) to 4000 nL/L near the bottom (178 nM/L) [69].

The Odoptinskoye, Piltun–Astokhskoye, Lunsky, and other oil and gas fields have been discovered in the southeastern part of the North Sakhalin sedimentary basin. The deposits are located in the zone of influence of the northern link of the Hokkaido–Sakhalin deep fault, which stretches through a narrow band of intense folded and discontinuous dislocations along the eastern coast of Sakhalin [57,64–72]. The deep faults of the region create a permeable geological environment for fluids.

In addition, there is the Daginsky gas-geothermal system of thermomineral waters [73, 74] on the coast in the coastal swampy area of the Nyysky Bay of the Sea of Okhotsk. Thermal springs are spatially common for the fault zone of the northeastern strike and the shallow ruptures of the eastern and southeastern strike that support it [75]. Another thermal manifestation is located in the northeastern part of Sakhalin Island 90 km south of the Daginsky gas-geothermal system on the western shore of the Lunsky Bay, at the mouth of the Kavle River valley. The hydrotherms are confined to the quaternary formations composing the coast of the Lunsky Bay. The Lunsky thermal springs are similar to the Daginsky ones according to their physico-chemical characteristics and geological conditions of formation. The cessation of the Lunsky thermal waters reaching the surface was noted in June 2014; however, gas bubbles were noted in the coastal part [76].

The author [57] allocates the territory of the southeastern part of Northern Sakhalin and the water area of the adjacent shelf to the Daginsky oil- and gas-bearing region. The presence of a significant clay fluid trap that overlaps the productive Daginsky strata is the key factor for oil and gas accumulation in the area. One favorable feature is the presence of permeable zones—the Hokkaido–Sakhalin, Pogranichny, and Mynginsk faults and the disjunctives supporting them—where various types of structural traps are formed.

5. Results and Discussion

A CTD survey with sampling of seawater consisted of three sections in the central part of the northeastern shelf of Sakhalin Island in the depth range of 4–300 m, implemented during cruise 68 of R/V Akademik Oparin (OP68) on 15–16 August 2023 (Table 1). The distance between the sampling points was about 10–15 km; the distance between the sections was 30 km.

A cold-water zone (5–6 °C) was observed along the coast of 30–50 km width (Figure 4a). The shelf front located along 100–150 m isobaths is a boundary between this cold shelf water and much warmer water (9–13 °C) of the open sea located over the shelf edge and slope. An origin of cold coastal water is probably associated with strong tidal mixing, which is known for the Sakhalin shelf area [38–40]. Coastal upwelling caused by southern winds dominating over this area in summer season [40,53] may also contribute to this cold-water zone. The distribution of salinity along the coast shows lower salinity in the north (31.4–31.7 psu), which may be considered as an influence of the Amur River water spreading along the Northwestern Sakhalin shelf down to 51–53 °N [40,54]. Low-salinity water may be also an impact of local lagoons. Water far from the coast has a higher salinity of up to 31.8–32.1 psu. Cold coastal water has higher turbidity (Figure 4c), with maximum values observed in the north. The highest concentration of chlorophyll-a was also found here (Figure 4d).

Water sampling to determine the content of dissolved gases, methane, carbon dioxide, helium, and hydrogen, were taken at 16 stations along three sections (Table 2, Figure 3). There are many local oil- and gas-bearing structures laying at up to 500 m depth in this area [57], and also, numerous manifestations of thermal waters are located on the northeastern coast of Sakhalin Island as Daginsky, Lunsky, and Paromay thermal springs [73–76].

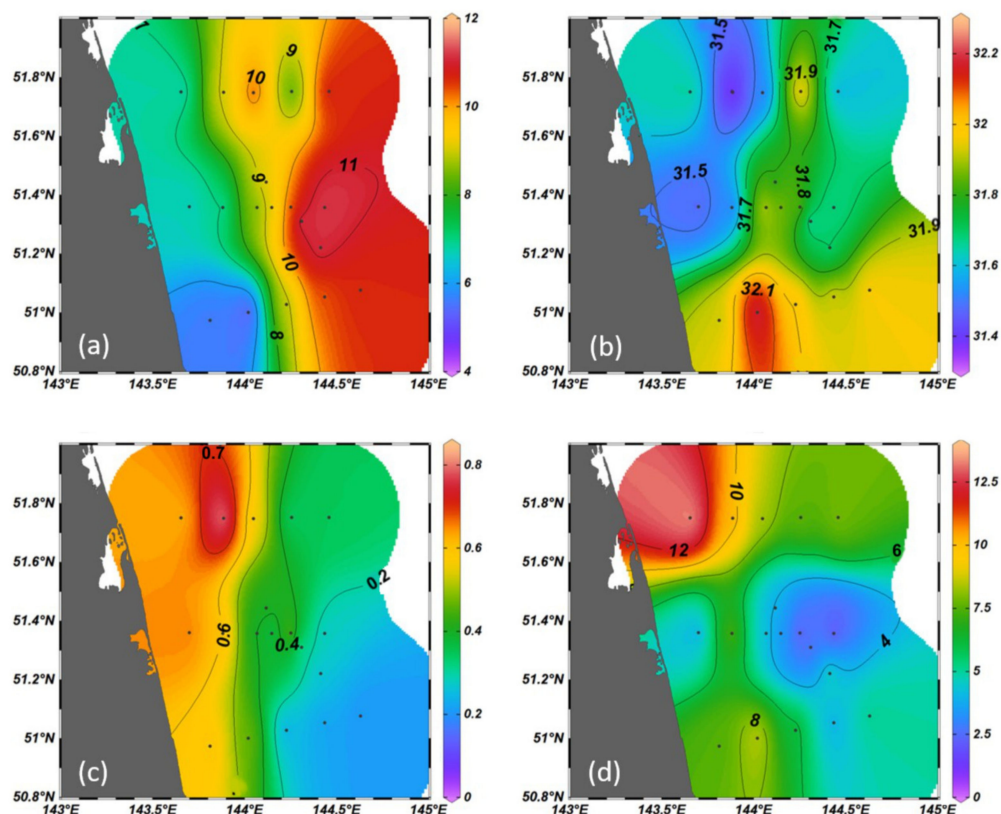


Figure 4. Distribution of (a) water temperature, (b) salinity, (c) turbidity, and (d) chlorophyll-a content in the surface layer on 15–16 August 2023 as examined by CTD observations (R/V Akademik Oparin, cruise 68).

Table 2. Materials researched.

	CH ₄	CO ₂	He	H ₂
Water Samples, pcs	95	95		95
Total		285		

Predominance of methane with a content of more than 80% and its light isotopic composition $\delta^{13}\text{C-CH}_4$ -54.5 – 66% are common for thermal manifestations in this area of Sakhalin Island [77]. This suggests a biogenic origin of gases, but probably with the presence of a thermogenic component [69,77]. Isotopic composition of methane from well bore number 54 in the Central Sabinsk area ($\delta^{13}\text{C-CH}_4$ -47.7%) that is close to the Daginsky geothermal sources may indicate variability in the isotopic composition of carbon from reservoir gases and surface gases.

Oil- and gas-containing rocks extending into the area of Daginsky geothermal springs [57] is the source of methane here, and the submeridional Hokkaido–Sakhalin fault zone control it, providing active fluid dynamics of the subsurface.

High concentrations of helium in water—up to 30 ppm [77]—are common for thermal springs of the northeastern coast of Sakhalin (Daginsky, Lunsky, Paromay thermal springs) due to their position in the zone of influence of the Hokkaido–Sakhalin fault system.

The CH₄/He ratio also indicates that warmer thermal waters actually stimulate methane production because of microbial processes. The isotopic and geochemical characteristics of the thermal waters of the Sakhalin coast are similar to those for sediment cores sampled in the area of gas-saturated sediments along the Kuril Basin [77].

The research area lies within the shallow shelf to 300 m depths and captures the oil- and gas-bearing structures of the Lunsky and Kirinsky gas condensate fields (see Figure 3).

The Lunskey gas condensate field is located within the northeastern shelf east of the northern closure of the Lunskey Bay of Sakhalin Island, 12–15 km from the coast. The sea depth in the field area is 45–50 m. The structural trap is a disturbed anticline extending along a line running approximately in a north-northwest direction. The deposit is divided into six main tectonic blocks with grabens in the northern part. Minor disturbances are also present within the main tectonic blocks.

The Kirinsky gas condensate field is also located on the northeastern shelf of Sakhalin Island. The Kirinsky Marine Area is located at a distance of 29 km from the coast and 15 km east of the Lunskey field. The depth of the sea in the field varies between 85 and 95 m.

A gas anomaly with a local methane maximum of 230 nM/L was detected at the bottom (at 45 m level) at the extreme western stations 32 and 33 within the northern section (Figure 5a); it is likely associated with a local gas emission. At the same time, methane spreads under the lower boundary of the seasonal pycnocline (10 m). This methane anomaly spreads to the east, and its concentrations decrease to 10 nM/L as they move away from its source and with increasing sea depth.

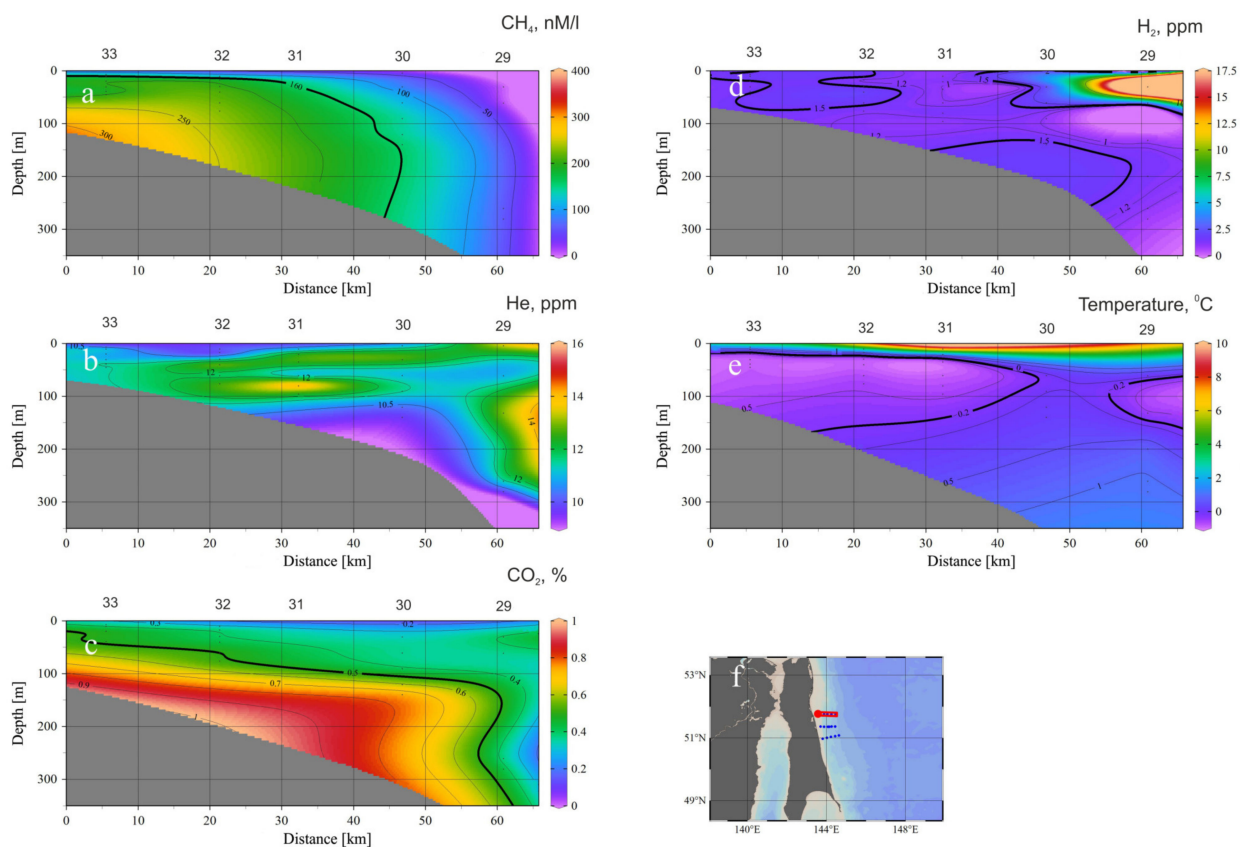


Figure 5. Methane (a), helium (b), carbon dioxide (c), hydrogen (d), and temperature (e) distribution in the northern section (f).

We also detected elevated helium concentrations of up to 11 ppm (Figure 5b). This inert gas can only be formed because of deep processes. For comparison, background helium concentrations in the Sea of Okhotsk (Kuril Basin area) are 4 ppm [78].

The carbon dioxide content in the bottom water does not exceed 1% (Figure 5c). The studies of [78,79] note the absence of CO₂ inflow from the mantle and point out that intrusive complexes do not influence the gas flow here. The CO₂ content in water increases, possibly due to the microbial oxidation of methane and the release of carbon dioxide during the activity of methane-oxidizing microbes. Also, significant amounts of CO₂ could be derived from other potential processes, such as from high-temperature decarbonation reactions or from the biodegradation of oils [80,81]. Modern tectonic activity

in the area of the northeastern shelf of Sakhalin leads to high heat flow, magmatic activity, and increased seismicity [57]. Helium is highly soluble in water and is an indicator of the location and extent of tectonic faults. Such properties of He are known for both sea and land conditions [82–86].

We detected high hydrogen concentrations of up to 40 ppm at station 29 at a 30 m depth (Figure 5d). Background hydrogen concentrations for the Sea of Okhotsk (Kuril Basin area) are 2.1 ppm [78]. Increased hydrogen concentrations are likely to spread further away from the shelf, which is associated with active microbial production of free hydrogen in the photic layer of seawater [87]. The life cycle of phytoplankton in the coastal waters of eastern Sakhalin is greatly influenced by the dynamics of waters. Bio production processes sharply intensify with the development of coastal upwelling; they are most active at 10–25 m depth, which is apparently due to the depth of the seasonal pycnocline. Comparatively high biomass values were noted at up to 75 m depths [88].

The presence of H₂ could also indicate biodegradation of longer-chain hydrocarbons [89,90]. The area is characterized by a large number of intersecting faults that cross the entire sedimentary sequence. Gaseous and liquid hydrocarbons as well as helium and hydrogen can migrate from deep subsurface origins to the sediment–water interface.

A gas anomaly with a local methane maximum of 295 nM/L and helium concentration of 16 ppm was detected at the bottom (at the level of 30 m and 84 m, respectively) within the central section at western stations 22 and 23 (Figure 6a,b). The increased carbon dioxide content in the water coincides with dissolved methane anomalies (Figure 6c). At the same time, methane spreads under the lower boundary of the seasonal pycnocline (10–40 m); its deepening in the central part of the section is associated with the influence of the East Sakhalin current. Elevated helium concentrations were detected at the sea bottom in the central (local maximum of 13.5 ppm) and eastern (absolute maximum of 17.2 ppm) parts of this section.

Probably, the dissolved gases migrate from the Sakhalin shelf towards its slope under the influence of the East Sakhalin current and mesoscale cyclones and anticyclones, which provide water exchange between the shelf and the deep-sea basin of the Sea of Okhotsk [44]. Such cyclonic circulation is one of the reasons for the increase in biological productivity on the northeastern shelf of Sakhalin in summer.

Local areas with increased hydrogen content of up to 15 ppm are located in the surface water layer of 20–30 m, which is also due to the fact that the eastern shelf of Sakhalin Island belongs to the waters with high biological production (Figure 6d).

A gas anomaly with local methane (225 nM/L) and helium (11.3 ppm) maxima was detected at the bottom (at the level of 161 m, 126 m, and 67 m, respectively) within the southern section at western stations 19, 20, and 21 (Figure 7a,b). At the same time, dissolved methane spreads under the lower boundary of the seasonal pycnocline (15–60 m), and its deepening in the central part of the section is associated with the influence of the East Sakhalin current. At the same time, increased carbon dioxide content in water correlates with anomalies of dissolved methane (Figure 7c).

These local areas of increased methane and helium concentrations are explained by high tectonic deformation and, as a result, areal methane release over oil- and gas-bearing structures through a network of faults.

High methane concentrations obtained in water are also confirmed by previous studies in this part of the Sakhalin shelf. The highest methane concentration of 10,900 nL/L or 487 nM/L, exceeding the background by two orders, was found in the bottom layer of seawater in the Lunsky area. High methane concentrations of 2000–3000 nL/L or 89–140 nM/L were found in the bottom water in the areas of open oil and gas fields—Odoptinsky, Piltun–Okhotsky, and others [14]. These methane concentrations exceed the background by two orders, and the background methane concentration in this area does not exceed 90–100 nL/L or 4–4.5 nM/L [71].

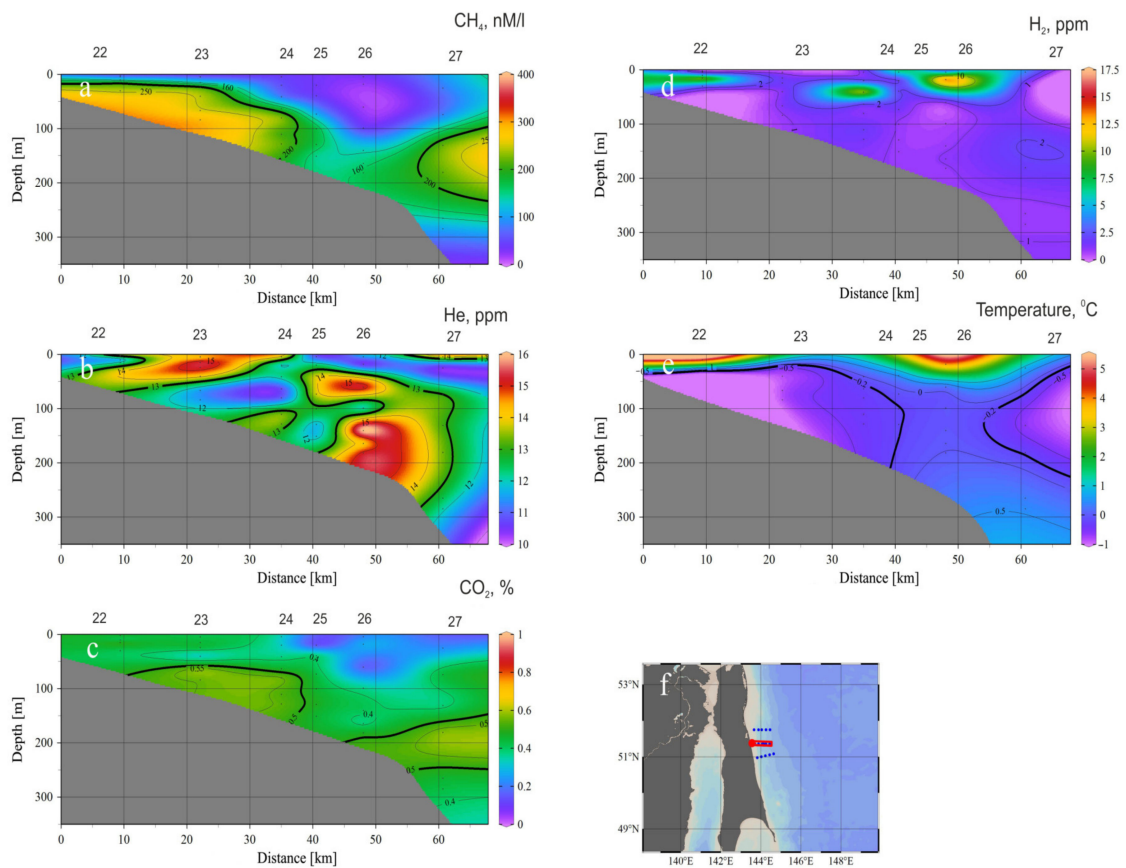


Figure 6. Methane (a), helium (b), carbon dioxide (c), hydrogen (d), and temperature (e) distribution in the central section (f).

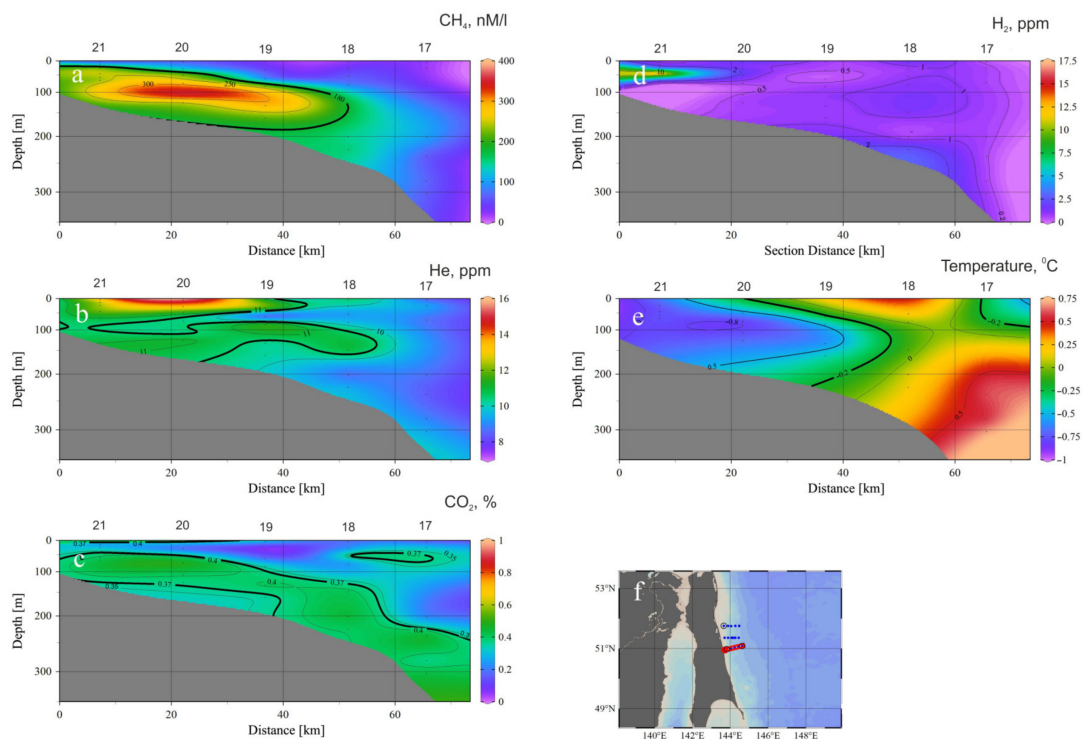


Figure 7. Methane (a), helium (b), carbon dioxide (c), hydrogen (d), and temperature (e) distribution in the southern section (f).

Our earlier studies established a very high methane concentration in the bottom layer of the entire area of the Kirinsky structure—from 2500 to 74,000 nL/L or from 110 to 3300 nM/L. That is, methane concentrations in the bottom layer on the Kirinsky structure exceed the background by 10–100 times or more. Streams of gas bubbles have been detected in the area of bore wells.

The northeastern Sakhalin shallow shelf is related to the transform boundary [57]. Modern high seismic activity and active faults that break through the sea floor [64] create a perfect gas-permeable state along this border. Anomalously high ambient methane and helium concentrations in the water column reflect that situation geochemically. Seismotectonic activity can cause intensive upward migration of methane, helium, and hydrogen from these deposits, generating secondary accumulations. Hydrogen and helium migrate together with methane through channels of vertical gas migration—a regional deep fault, with a network of submeridian faults (see Figure 3). Helium is concentrated in hydrocarbon fluids circulating in the fault zone. Therefore, tectonic faults, especially their intersections, are recorded by helium anomalies in the water column.

We also performed a comparison of remote sensing data with the results of expedition studies. It shows the spatial distribution of methane near the surface in the research area and on the nearest coast (Figure 8A).

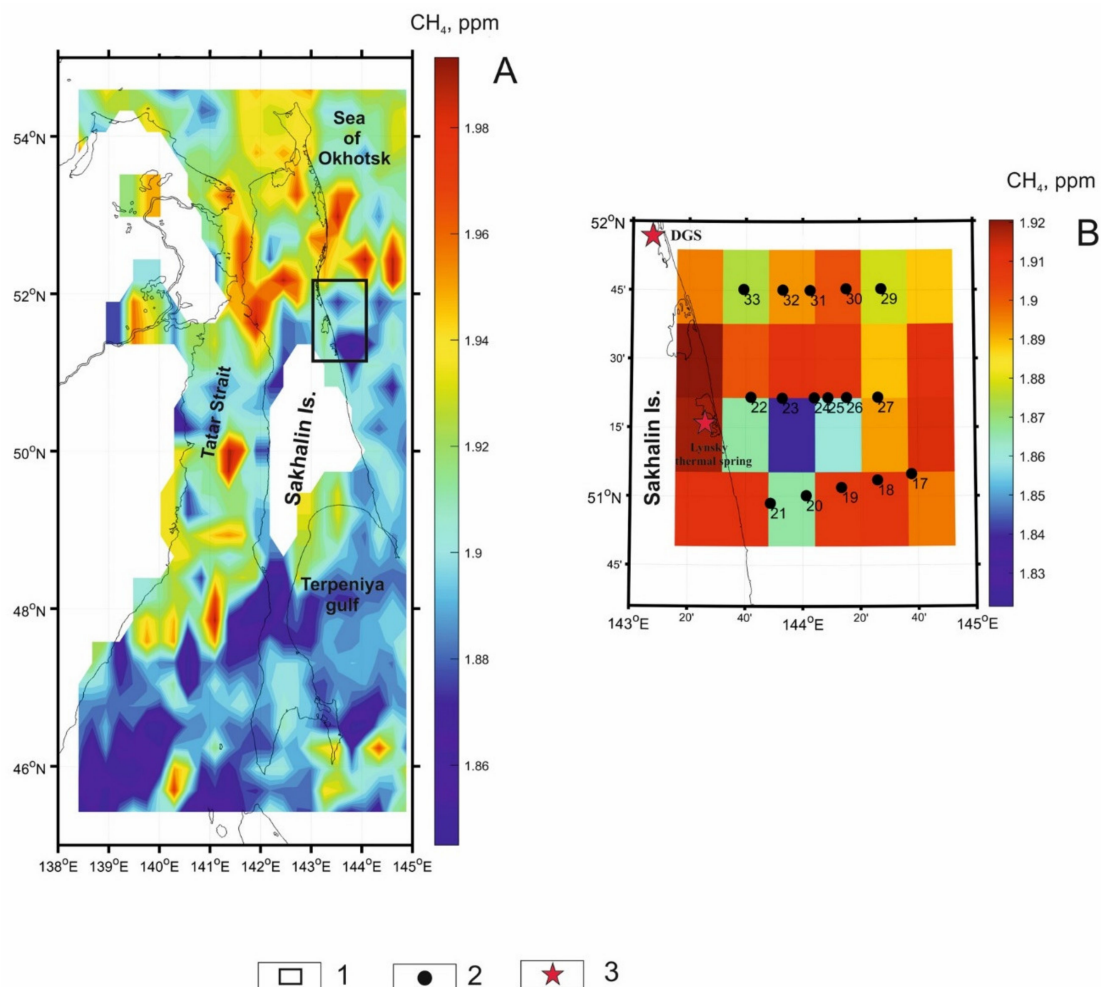


Figure 8. Spatial distribution of methane concentrations according to the AIRS scanner data above the surface for the period of 15–16 August 2023. (A) is the distribution of methane concentrations above the surface of Sakhalin and its shelf; (B) is distribution of methane concentrations above the surface in the research area. 1—Research area; 2—water sampling stations in cruise OP68; 3—thermal springs (DGS—Daginsky gas-geothermal system, Linsky thermal spring).

The research area (Figure 8B) is generally characterized by increased concentrations of methane in the air layer above the water surface. The distribution of methane on the northeastern shallow shelf of Sakhalin is heterogeneous, which is mainly due to the location of underwater methane sources and thermal springs on the coast. This is also explained by the complex current structure and seasonal changes in the hydrological regime. As a result, the heterogeneous distribution of methane in seawater is associated with the processes of methane release and absorption at the water–atmosphere boundary.

Gas migration from its lithospheric sources (oil and gas deposits, gas-saturated sediments, mud volcanism) controls methane distribution near the surface of the water area and the nearest coast, as well as the distribution of methane in the water column. Methane concentrations are likely to increase under the influence of higher wind speeds and higher water temperatures. The combination of tectonic conditions, the distribution of oil- and gas-bearing structures and a special hydrological regime, including the formation of mesoscale vortices in addition to the main flow of the East Sakhalin current, are the leading factors determining the formation and distribution of methane, helium, and hydrogen in the area of the northeastern shallow shelf of Sakhalin Island.

Thus, large amounts of gases from oil- and gas-bearing structures, which are affected by faults, are released into the sea-water column, results in the origin of both seawater dissolved methane and helium anomalies found in the water column over the northeastern shallow of the North Sakhalin trough. Methane moves from the depths into the water through fault zones and cracks and saturates the entire water column on the shallow shelf. The oil and gas content in rocks on the Sakhalin shelf decreases with depth, so the ability to supply methane from bottom rocks into the water of the deep-water shelf and slope will decrease. Furthermore, during the development of coastal upwelling and associated mesoscale circulations, dissolved gases are transported from the shelf to the east under the lower boundary of the seasonal pycnocline into the deep part of the Sea of Okhotsk and are involved in its general circulation. Therefore, studies of the shallow-water oil and gas shelf are necessary to understand the processes of methane emission to the atmosphere as well as the nature of modern climate change.

6. Conclusions

We presented the first measurements of helium and hydrogen in the water column in the area of the shallow northeastern shelf of Sakhalin. Underlying rocks, reservoirs of oil- and gas-containing fluids, are the sources of methane in the studied area. The oil- and gas-bearing rocks cover not only the shelf, but also include significant coastal areas of the island, where numerous thermal springs with a predominance of methane in the gas composition are located.

The coincidence of methane and helium anomalies confirms the gas emission from hydrocarbon deposits under the sea bottom subsurface into the seawater through fault zones and cracks. Tectonic faults in the northeastern part of Sakhalin Island and the adjacent shelf adjust oil and gas deposits, coastal thermal springs, abnormal methane and helium concentrations, as well as elevated carbon dioxide concentrations.

The conducted gas-geochemical studies indicate the presence of intensive sources of gas emission in the shallow northeastern shelf of Sakhalin Island. Measured methane content is very high at 200–400 nM/L, and helium content is rather high, 8–18 ppm, for the bottom water layers. The content of dissolved gases in the water increases from east to west, towards the coast, due to an increase in the oil and gas content of rocks from the slope to the shallow shelf and to the complex hydrological regime of the area.

High methane concentrations are observed throughout the water column from the bottom to the surface over the shallow shelf (up to 20–30 m depth), which is probably due to convective mixing of water. As a result, bottom waters saturated with methane rise to the surface. The main methane emission from the water into the atmosphere occurs in the area of the shallow northeastern shelf.

The combined influence of the East Sakhalin current and counter-current makes dissolved gases be transported under the lower boundary of the seasonal pycnocline from the shelf to the east into the deep water part of the Sea of Okhotsk, and they are involved in its general circulation. Low water temperatures in the study area ensure a high level of solubility of gases released from bottom sources.

Author Contributions: Conceptualization, N.S. and A.K.; data curation, V.L.; formal analysis, N.S.; funding acquisition, N.S. and V.L.; methodology, N.S. and I.S.; validation, N.S. and S.S.; visualization, A.K. and I.S.; writing—original draft, A.K.; writing—review and editing, N.S. All authors have read and agreed to the published version of the manuscript.

Funding: This research was funded by a Russian Science Foundation grant No. 23-77-10038, <https://rscf.ru/project/23-77-10038/> (accessed on 14 August 2023).

Data Availability Statement: Data is contained within the article.

Acknowledgments: The authors thank the research group and the crew of cruise 68 of the R/V Akademik Oparin, and they especially thank Aleksandr Sergeev and Pavel Semkin for organizing deck work and efficient observations and sampling.

Conflicts of Interest: The authors declare that they have no known competing financial interests or personal relationships that could have appeared to influence the work reported in this paper.

References

- Shakirov, R.B. *Gasgeochemical Fields of the Eastern Asia Marginal Seas*; GEOS: Moscow, Russia, 2018; 341p.
- Grannik, V.M. Comparison of structural elements of Sakhalin and Hokkaido. *Dokl. Earth Sci.* **2005**, *401*, 177–181. (In Russian)
- Grannik, V.M. The East-Sakhalin island arc system of the Okhotsk Sea region. *Litosfera* **2013**, *1*, 36–51. (In Russian)
- Rozhdestvenskiy, V.S. Evolution of the Sakhalin folds system. *Tectonophysics* **1986**, *127*, 331–339. [[CrossRef](#)]
- Khanchuk, A.I. The Geological Structure and Evolution of the Continental Surroundings of the NW Pacific Ocean. Ph.D. Thesis, Geological Institute of the Academy, Moscow, Russia, 1993; p. 31.
- Chekhovich, V.D. *The Tectonics and Geodynamics of the Folded Surroundings of Small Oceanic Basins*; Nauka: Moscow, Russia, 1993; p. 272.
- Isozaki, Y. Anatomy and genesis of a subduction-related orogen: A new view on the geotectonic subdivision and evolution of the Japanese Islands. *Isl. Arc* **1996**, *5*, 289. [[CrossRef](#)]
- Maruyama, S.; Isozaki, Y.; Kimura, G.; Terabayashi, M. Paleogeographic maps of the Japanese Islands: Plate tectonic synthesis from 750 Ma to the present. *Isl. Arc* **1997**, *6*, 121. [[CrossRef](#)]
- Zharov, A.E. South Sakhalin tectonics and geodynamics: A model for the Cretaceous–Paleogene accretion of the East Asian continental margin. *Russ. J. Earth. Sci.* **2005**, *7*, ES5002. [[CrossRef](#)]
- Zlobin, T.K.; Bobkov, A.O. *Modern Seismicity and Fault Tectonics of the South of Sakhalin*; Publishing house of SAKHGU: Yuzhno-Sakhalinsk, Russia, 2003; 124p. (In Russian)
- Earthquake Hazards Program. Available online: <https://earthquake.usgs.gov> (accessed on 20 February 2024).
- Avdeiko, G.P.; Gavrilenko, G.M.; Chertkova, L.V.; Bondarenko, V.I.; Rashidov, V.A.; Guseva, V.I.; Maltseva, V.I.; Sazonov, V.I. and others. Underwater gas hydrothermal activity on the northwestern slope of Paramushir Island (Kuril Islands). *Volcanol. Seismol.* **1984**, *6*, 66–81. (In Russian)
- Ginsburg, G.D.; Soloviev, V.A.; Cranston, R.E.; Lorenson, T.D.; Kvenvolden, K.A. Gas hydrates from continental slope, offshore Sakhalin Island, Okhotsk Sea. *Geo-Mar. Lett.* **1993**, *13*, 41–48. [[CrossRef](#)]
- Obzhairov, A.I. Gasgeochemical manifestation of gas hydrates in the Sea of Okhotsk. *Alsk. Geol.* **1992**, *21*, 1–7.
- Lammers, S.; Suess, E.; Mansurov, M.N.; Anikiev, V.V. Variations of atmospheric methane supply from the Sea of Okhotsk induced by seasonal ice cover. *Glob. Biogeochem. Cycle* **1995**, *9*, 351–358. [[CrossRef](#)]
- Heggland, R. Gas seepage is an indicator of deeper prospective reservoirs. A study based on exploration 3D seismic data. *Mar. Pet. Geol.* **1998**, *15*, 1–9. [[CrossRef](#)]
- Hagen, R.A.; Vogt, P.R. Seasonal variability of shallow biogenic gas in Chesapeake Bay. *Mar. Geol.* **1999**, *158*, 75–88. [[CrossRef](#)]
- Etiopie, G.; Italiano, F.; Fuda, L.; Favali, P.; Frugoni, F.; Calcara, M.; Smriglio, G.; Gamberi, F.; Marani, M. Deep Submarine Gas Vents in the Aeolian Offshore. *Phys. Chem. Earth Part B Hydrol. Ocean. Atmos.* **2000**, *25*, 25–28. [[CrossRef](#)]
- Lorenson, T.D.; Kvenvolden, K.A.; Hostettler, F.D. Hydrocarbon geochemistry of cold seeps in the Monterey Bay. *Mar. Geol.* **2002**, *181*, 285–304. [[CrossRef](#)]
- Obzhairov, A.I.; Ilyichev, V.I.; Kulinich, R.G. Anomaly of natural gases in bottom water. *DAN USSR* **1985**, *281*, 1206–1209. (In Russian)
- Kulinich, R.G.; Obzhairov, A.I. Structure and modern activity of the joint zone of the Sunda shelf and the South China Sea basin. *Pac. Geol.* **1985**, *3*, 102–106.
- Abrams, M. Geophysical and geochemical evidence for subsurface hydrocarbon leakage in the Bering Sea, Alaska. *Mar. Petrol. Geol.* **1992**, *9*, 208–221. [[CrossRef](#)]

23. Hovland, M.; Croker, P.F.; Martin, M. Fault—Associated seabed mounds (carbonate knolls?) off western Ireland and north-west Australia. *Mar. Pet. Geol.* **1994**, *11*, 232–246. [[CrossRef](#)]
24. Mau, S.; Tu, T.-H.; Becker, M.; dos Santos Ferreira, C.; Chen, J.-N.; Lin, L.-H.; Wang, P.-L.; Lin, S.; Bohrmann, G. Methane Seeps and Independent Methane Plumes in the South China Sea Offshore Taiwan. *Front. Mar. Sci.* **2020**, *7*, 543. [[CrossRef](#)]
25. Mau, S.; Valentine, D.; Clark, J.F.; Reed, J.; Camilli, R.; Washburn, L. Dissolved methane distributions and air-sea flux in the plume of a massive seep field, Coal Oil Point, California. *Geophys. Res. Lett.* **2007**, *34*, L22603. [[CrossRef](#)]
26. Shakirov, R.B.; Valitov, M.G.; Obzhirov, A.I.; Mishukov, V.F.; Yatsuk, A.V.; Syrbu, N.S.; Mishukova, O.V. Methane anomalies, its flux on the sea–atmosphere interface and their relations to the geological structure of the South-Tatar sedimentary basin (Tatar Strait, the Sea of Japan). *Mar. Geophys. Res.* **2019**, *40*, 581–600. [[CrossRef](#)]
27. Mishukova, G.; Yatsuk, A.; Shakirov, R.; Syrbu, N.; Valitov, M.; Ponomareva, A.; Mishukova, O. Methane Fluxes at the Water–Atmosphere Interface and Gas-Geochemical Anomalies in the Bottom Sediments in the Northwestern Part of the Sea of Japan. *Russ. Geol. Geophys.* **2021**, *62*, 1385–1400. [[CrossRef](#)]
28. Yatsuk, A.; Shakirov, R.; Gresov, A.; Obzhirov, A. Hydrocarbon gases in seafloor sediments of the TATAR strait, the northern sea of Japan. *Geo-Mar. Lett.* **2019**, *40*, 481–490. [[CrossRef](#)]
29. Snyder, G.T.; Yatsuk, A.; Takahata, N.; Shakirov, R.; Tomaru, H.; Tanaka, K.; Obzhirov, A.; Salomatin, A.; Aoki, S.; Khazanova, E.; et al. Ocean Dynamics and Methane Plume Activity in Tatar Strait, Far Eastern Federal District, Russia as Revealed by Seawater Chemistry, Hydroacoustics, and Noble Gas Isotopes. *Front. Earth Sci.* **2021**, *10*, 825679. [[CrossRef](#)]
30. Mau, S.; Heintz, M.B.; Valentine, D.L. Quantification of CH₄ loss and transport in dissolved plumes of the Santa Barbara Channel, California. *Cont. Shelf Res.* **2012**, *32*, 110–120. [[CrossRef](#)]
31. Rehder, G.; Keir, R.S.; Suess, E.; Pohlman, T. The multiple sources and patterns of methane in North Sea waters. *Aquat. Geochem. Kluwer Acad. Publ.* **1998**, *4*, 403–427. [[CrossRef](#)]
32. Cynar, F.J.; Yayanos, A.A. The distribution of methane in upper waters of the Southern California Bight. *J. Geophys. Res.* **1992**, *97*, 11269–11285. [[CrossRef](#)]
33. Vereshchagina, O.F.; Korovitskaya, E.V.; Mishukova, G.I. Methane in water columns and sediments of the north western Sea of Japan. *Deep. Sea Res. Part II Top. Stud. Oceanogr.* **2013**, *86–87*, 25–33. [[CrossRef](#)]
34. Yamamoto, S.; Alcauskas, J.B.; Crozier, T.E. Solubility of methane in distilled water and sea water. *J. Chem. Eng. Data* **1976**, *21*, 78–80. [[CrossRef](#)]
35. Wiesenburg, D.A.; Guinasso, N.L. Equilibrium solubility of methane, carbon monoxide, and hydrogen in water and sea water. *J. Chem. Eng. Data* **1979**, *24*, 356–360. [[CrossRef](#)]
36. AIRS/AMSU/HSB Version 7 Level 2 Product User Guide. Available online: https://docserver.gesdisc.eosdis.nasa.gov/public/project/AIRS/V7_L2_Product_User_Guide.pdf (accessed on 5 March 2024).
37. Atmospheric InfraRed Sounder (AIRS). Available online: <https://airs.jpl.nasa.gov/> (accessed on 5 March 2024).
38. Leonov, A.K. *Regional Oceanography*; Hydrometeoizdat: Leningrad, Russia, 1960; p. 165. (In Russian)
39. Vlasova, G.A.; Glebova, S.Y. Seasonal variability of surface currents of the Sea of Okhotsk under the influence of synoptic processes. *Izv. TINRO* **2008**, *154*, 259–269.
40. Vlasova, G.A.; Vasiliev, A.S.; Shevchenko, G.V. *Spatial and Temporal Variability of the Water Structure and Dynamics of the SEA of Okhotsk*; Nauka: Moscow, Russia, 2008; 359p. (In Russian)
41. Luchin, V.A. Nonperiodical currents. In *Hydrometeorology and Hydrochemistry of the seas. V. 9. The Okhotsk Sea, P. 1. Hydrometeorological Conditions*; Glukhovskoy, B.K., Goptarev, N.P., Terziev, F.S., Eds.; Gidrometeoizdat: St. Petersburg, Russia, 1998; pp. 232–256.
42. Ohshima, K.I.; Wakatsuchi, M.; Fukamachi, Y.; Mizuta, G. Near-surface circulation and tidal currents of the Okhotsk Sea observed with satellite-tracked drifters. *J. Geophys. Res.* **2002**, *107*, C11. [[CrossRef](#)]
43. Talley, L.D. An Okhotsk Sea water anomaly: Implications for ventilation in the North Pacific. *Deep-Sea Res.* **1991**, *38* (Suppl. S1), S171–S190. [[CrossRef](#)]
44. Luchin, V.A. Circulation of the waters of the Sea of Okhotsk and features of its intra-annual variability according to the results of diagnostic calculations. *Trudy DVNII* **1987**, *36*, 3–13. (In Russian)
45. Vasiliev, A.S.; Khrapchenkov, F.F. Seasonal variability of water circulation and water exchange of the Sea of Okhotsk with the Pacific Ocean. *Meteorol. Hydrol.* **1998**, *6*, 59–67. (In Russian)
46. Simizu, D.; Ohshima, K.I. Barotropic Response of the Sea of Okhotsk to Wind Forcing. *J. Oceanogr.* **2002**, *58*, 851–860. [[CrossRef](#)]
47. Shimada, Y.; Kubokawa, A.; Ohshima, K. Influence of Current Width Variation on the Annual Mean Transport of the East Sakhalin Current: A Simple Model. *J. Oceanogr.* **2005**, *61*, 913–920. [[CrossRef](#)]
48. Simizu, D.; Ohshima, K.I. A model simulation on the circulation in the Sea of Okhotsk and the East Sakhalin Current. *J. Geophys. Res.* **2006**, *111*, C05016. [[CrossRef](#)]
49. Ohshima, K.I.; Simizu, D. Particle tracking experiments on a model of the Okhotsk Sea: Toward oil spill simulation. *J. Oceanogr.* **2008**, *64*, 103–114. [[CrossRef](#)]
50. Ebuchi, N. Seasonal and interannual variations in the East Sakhalin Current revealed by the TOPEX/POSEIDON altimeter data. *J. Oceanogr.* **2006**, *62*, 171–183. [[CrossRef](#)]
51. Fayman, P.A. *Atlas of the Sea of Okhotsk*; Far Eastern Regional Hydrometeorological Research Institute (FERHRI): Vladivostok, Russia, 2018; p. 133. (In Russian)

52. Fayman, P.; Prants, S.; Budyansky, M.; Uleysky, M. New Circulation Features in the Okhotsk Sea from a Numerical Model. *Izv. Atmos. Ocean. Phys.* **2020**, *56*, 618–631. [[CrossRef](#)]
53. Rybalko, S.I.; Shevchenko, G.V. Seasonal and spatial variability of sea currents on the Sakhalin northeastern shelf. *Pac. Oceanogr.* **2003**, *1*, 168–178.
54. Pishchalnik, V.M.; Arkhipkin, V.S.; Leonov, A.V. Vosstanovleniye godovogo khoda termokhalinnykh kharakteristik i tsirkulyatsii vod na severo-vostochnom shel'fe Sakhalina (Reconstruction of the annual course of thermohaline characteristics and water circulation on the northeastern shelf of Sakhalin). *Water Resour.* **2014**, *41*, 362–374. (In Russian)
55. Fayman, P.A.; Prants, S.V.; Budyansky, M.V.; Uleysky, M.Y. Simulated Pathways of the Northwestern Pacific Water in the Okhotsk Sea. *Izv. Atmos. Ocean. Phys.* **2021**, *57*, 329–340. [[CrossRef](#)]
56. Prants, S.; Andreev, A.; Budyansky, M.; Uleysky, M. Mesoscale circulation along the Sakhalin Island eastern coast. *Ocean. Dyn.* **2016**, *67*, 345–356. [[CrossRef](#)]
57. Kharakhinov, V.V. *Oil and Gas Geology of the Sakhalin Region*; Scientific World: Moscow, Russia, 2010; 276p. (In Russian)
58. Zonenshain, L.P.; Savostin, L.A. *Introduction to Geodynamics*; Nedra: Moscow, Russia, 1979; 311p. (In Russian)
59. Ulomov, V.I. On the Main Provisions and Technical Recommendations for the Creation of a New Map of Seismic Zoning of the Territory of the Russian Federation. In *Seismicity and Seismic Zoning of Northern Eurasia*; OIF RAS: Moscow, Russia, 1995; pp. 6–26. (In Russian)
60. Rozhdestvenskiy, V.S. On shear displacements along the Tym-Poronai fault zone on Sakhalin Island. *DAN USSR* **1976**, *230*, 678–780.
61. Shakirov, R.B.; Syrbu, N.S. Natural Sources of Methane and Carbon Dioxide on Sakhalin Island and Their Role in the Formation of Ecological Gas-Geochemical Zones. *Water Resour.* **2013**, *40*, 752–760. [[CrossRef](#)]
62. Syrbu, N.S.; Kholmogorov, A.O.; Steepochkin, I.E.; Khazanova, E.S. Comparative Analysis of Gas-Geochemical Data from Ground-Based and Satellite Observations of the Sakhalin Island and Its Shelf (Northeast Russia): Tectonic Consequences. *Geotectonics* **2023**, *57*, 184–199. [[CrossRef](#)]
63. Voeikova, O.A.; Nesmeyanov, S.A.; Serebryakova, L.I. *Neotectonics and Active Faults of Sakhalin*; (In Russian). Nauka: Moscow, Russia, 2007; 187p. (In Russian)
64. Baranov, B.V.; Rukavishnikova, D.D.; Prokudin, V.G.; Jin, Y.K.; Dozorova, K.A. The origin of enclosed depressions on the eastern Sakhalin slope. *Vestn. Kamchat. Reg. Assots. Ser. Nauki Zemle* **2013**, *1*, 86–97.
65. Baranov, B.V.; Karp, B.Y.; Wong, H.K. *Areas of Gas Seepage*; KOMEX Cruise Report I RV Professor Gagarinsky, Cruise 22. GEOMAR Report 82 INESSA; GEOMAR: Kiel, Germany, 1999; pp. 45–52.
66. Baranov, B.; Karp, B.; Karnaukh, V. *Western Okhotsk Sea: Multifarious Tectonic Structure*; Geomar Report 105 SERENADE. RV Professor Gagarinsky, Cruise 32; GEOMAR: Kiel, Germany, 2002; pp. 32–40.
67. Sim, L.A.; Kamenev, P.A.; Bogomolov, L.M. New data on the latest stress state of the earth's crust on Sakhalin Island (based on structural and geomorphological indicators of tectonic stress). *Geosyst. Transit. Zones* **2020**, *4*, 372–383, (In Russian, Abstract in English). [[CrossRef](#)]
68. Nikolaevskii, V.N.; Ramazanov, T.K. Generation and propagation of waves along deep faults. *Izv. Akad. Nauk SSSR Fiz. Zemli* **1986**, *10*, 3–13.
69. Shakirov, R.; Obzhairov, A.; Suess, E.; Salyuk, A.; Nicole, B. Mud volcanoes and gas vents in the Okhotsk Sea area. *Geo-Marine Letters* **2004**, *24*, 140–149. [[CrossRef](#)]
70. Shakirov, R.B.; Obzhairov, A.I.; Biebow, N.; Salyuk, A.N.; Tsunogai, U.; Terekhova, V.E.; Shoji, H. Classification of anomalous methane fields in the Okhotsk Sea. *Polar Meteorol. Glaciol.* **2005**, *19*, 50–66.
71. Obzhairov, A.I.; Shakirov, R.; Salyuk, A.; Suess, E.; Biebow, N.; Salomatin, A. Relations between Methane Venting, Geological Structure and Seismo-Tectonics in the Okhotsk Sea. *Geo-Mar. Lett.* **2004**, *24*, 135–139. [[CrossRef](#)]
72. Baranov, B.V.; Dozorova, K.A.; Rukavishnikova, D.D. Hazardous geological processes on the eastern slope of Sakhalin. *Oceanology* **2015**, *55*, 906–909. [[CrossRef](#)]
73. Zharkov, R.V. Temperature regime of the Darginsky thermal springs (Sakhalin Island) during their reconstruction in 2019–2021. *IOP Conf. Ser. Earth Environ. Sci.* **2021**, *946*, 012032. [[CrossRef](#)]
74. Nikitenko, O.A.; Ershov, V.V.; Zharkov, R.V.; Ustyugov, G.V. Temperature and chemical composition of thermos-mineral water from Darginsky sources (Sakhalin Island) after reconstruction of the capitation structures in 2019–2020. *Vestn. Kamchat. Reg. Assots., Ser. Nauki Zemle* **2023**, *2*, 58. [[CrossRef](#)]
75. Zharkov, R.V. Modern physicochemical features of thermomineral water of the Darginsky deposit (Sakhalin Island). *Monitoring. Sci. Technol.* **2018**, *4*, 35–40. (In Russian) [[CrossRef](#)]
76. Zharkov, R.V. Physical and chemical properties of thermal waters of the Lunsyky springs (Sakhalin Island). *Geosyst. Transit. Zones* **2019**, *3*, 249–255. [[CrossRef](#)]
77. Syrbu, N.S.; Snyder, G.T.; Shakirov, R.B.; Kholmogorov, A.O.; Zharkov, R.V.; Tsunogai, U. Geochemical distribution of helium, hydrogen, carbon dioxide, and methane in Sakhalin Island mud volcanoes, hot springs, and cold seeps. *J. Volcanol. Geotherm. Res.* **2022**, *431*, 107667. [[CrossRef](#)]
78. Shakirov, R.B.; Syrbu, N.S.; Obzhairov, A.I. Distribution of helium and hydrogen in sediments and water on the Sakhalin slope. *Lithol. Miner. Resour.* **2016**, *511*, 61–73. [[CrossRef](#)]

79. Lavrushin, V.Y.; Polyak, B.G.; Prasolov, R.M.; Kamenskii, I.L. Sources of material in mud volcano products (Based on Isotopic, hydrochemical, and geological data). *Lithol. Miner. Resour.* **1996**, *316*, 557–578.
80. Head, I.M.; Jones, D.M.; Larter, S.R. Biological activity in the deep subsurface and the origin of heavy oil. *Nature* **2003**, *426*, 344–352. [[CrossRef](#)] [[PubMed](#)]
81. Etiope, G.; Feyzullayev, A.; Milkov, A.V.; Waseda, A.; Mizobe, K.; Sun, C.H. Evidence of subsurface anaerobic biodegradation of hydrocarbons and potential secondary methanogenesis in terrestrial mud volcanoes. *Mar. Pet. Geol.* **2009**, *269*, 1692–1703. [[CrossRef](#)]
82. Moraru, K.E. Tectonic features and the macroseismic field of the southwestern part of the Russian platform. *Russ. Seismol. J.* **2020**, *2*, 48–57. (In Russian) [[CrossRef](#)]
83. Baumberger, T.; Embley, R.W.; Merle, S.G.; Lilley, M.D.; Raineault, N.A.; Lupton, J.E. Mantle-Derived Helium and Multiple Methane Sources in Gas Bubbles of Cold Seeps Along the Cascadia Continental Margin. *Geochem. Geophys. Geosyst.* **2018**, *19*, 4476–4486. [[CrossRef](#)]
84. Boles, J.R.; Garven, G.; Camacho, H.; Lupton, J.E. Mantle helium along the Newport-Inglewood fault zone, Los Angeles basin, California: A leaking paleosubduction zone. *Geochem. Geophys. Geosyst.* **2015**, *16*, 2364–2381. [[CrossRef](#)]
85. Caracausi, A.; Paternoster, M. Radiogenic helium degassing and rock fracturing: A case study of the southern Apennines active tectonic region. *J. Geophys. Res. Solid Earth* **2015**, *120*, 2200–2211. [[CrossRef](#)]
86. McCrory, P.A.; Constantz, J.E.; Hunt, A.G.; Blair, J.L. Helium as a tracer for fluids released from Juan de Fuca lithosphere beneath the Cascadia fore arc. *Geochem. Geophys. Geosyst.* **2016**, *17*, 2434–2449. [[CrossRef](#)]
87. Tishchenko, P.P. Phytoplankton primary production on the northeastern Sakhalin Island shelf in summer. *Mar. Biol. J.* **2023**, *7*, 81–97. [[CrossRef](#)]
88. Obzhairov, A.I.; Sosnin, V.A.; Salyuk, A.N.; Vereshchagina, O.F.; Luchsheva, L.N.; Mishukova, G.I.; Astakhova, N.V.; Sorochinskaya, A.V.; Zakharkov, S.P.; Selina, M.S. (Eds.) *Methane Monitoring in the Sea of Okhotsk*; Dalnauka Publishing House: Vladivostok, Russia, 2002; 250p.
89. Charlou, J.L.; Donval, J.P.; Fouquet, Y.; Jean-Baptiste, P.; Holm, N. Geochemistry of high H₂ and CH₄ vent fluids issuing from ultramafic rocks at the Rainbow hydrothermal field (36°14' N, MAR). *Chem. Geol.* **2002**, *1914*, 345–359. [[CrossRef](#)]
90. Hassanpouryouzband, A.; Wilkinson, M.; Haszeldine, R.S. Hydrogen energy futures—Foraging or farming? *Chem. Soc. Rev.* **2024**, *53*, 2258–2263. [[CrossRef](#)] [[PubMed](#)]

Disclaimer/Publisher's Note: The statements, opinions and data contained in all publications are solely those of the individual author(s) and contributor(s) and not of MDPI and/or the editor(s). MDPI and/or the editor(s) disclaim responsibility for any injury to people or property resulting from any ideas, methods, instructions or products referred to in the content.